HHS Public Access

Author manuscript

Brain Struct Funct. Author manuscript; available in PMC 2015 May 01.

Published in final edited form as:

Brain Struct Funct. 2015 May ; 220(3): 1497–1509. doi:10.1007/s00429-014-0740-x.

The *Lhx9* homeobox gene controls pineal gland development and prevents postnatal hydrocephalus

Fumiyoshi Yamazaki,
Section on Neuroendocrinology, Program in Developmental Endocrinology and Genetics, The Eunice Kennedy Shriver National Institute of Child Health and Human Development, National Institutes of Health, 49 Convent Drive, Room 6A82, Bethesda, MD 20892-4510, USA

Morten Møller,
Department of Neuroscience and Pharmacology, Faculty of Health and Medical Sciences, University of Copenhagen, Copenhagen, Denmark

Cong Fu,
Section on Neuroendocrinology, Program in Developmental Endocrinology and Genetics, The Eunice Kennedy Shriver National Institute of Child Health and Human Development, National Institutes of Health, 49 Convent Drive, Room 6A82, Bethesda, MD 20892-4510, USA

Samuel J. Clokie,
Section on Neuroendocrinology, Program in Developmental Endocrinology and Genetics, The Eunice Kennedy Shriver National Institute of Child Health and Human Development, National Institutes of Health, 49 Convent Drive, Room 6A82, Bethesda, MD 20892-4510, USA

Artem Zykovich,
Section on Neuroendocrinology, Program in Developmental Endocrinology and Genetics, The Eunice Kennedy Shriver National Institute of Child Health and Human Development, National Institutes of Health, 49 Convent Drive, Room 6A82, Bethesda, MD 20892-4510, USA

Steven L. Coon,
Section on Neuroendocrinology, Program in Developmental Endocrinology and Genetics, The Eunice Kennedy Shriver National Institute of Child Health and Human Development, National Institutes of Health, 49 Convent Drive, Room 6A82, Bethesda, MD 20892-4510, USA

David C. Klein, and

D. C. Klein kleind@mail.nih.gov.
Present Address: F. Yamazaki Department of Cell Biology and Anatomy, Hamamatsu University School of Medicine, Hamamatsu, Shizuoka, Japan
Present Address: C. Fu State Key Laboratory of Theoretical and Computational Chemistry, Institute of Theoretical Chemistry, Jilin University Changchun, Jilin, China
Present Address: S. J. Clokie West Midlands Regional Genetics Laboratories, Birmingham Women's NHS Foundation Trust, Birmingham, UK
Present Address: A. Zykovich Buck Institute for Research on Aging, Novato, CA, USA

The authors declare no competing financial interests.

Electronic supplementary material The online version of this article (doi:10.1007/s00429-014-0740-x) contains supplementary material, which is available to authorized users.

Section on Neuroendocrinology, Program in Developmental Endocrinology and Genetics, The Eunice Kennedy Shriver National Institute of Child Health and Human Development, National Institutes of Health, 49 Convent Drive, Room 6A82, Bethesda, MD 20892-4510, USA

Martin F. Rath
Department of Neuroscience and Pharmacology, Faculty of Health and Medical Sciences, University of Copenhagen, Copenhagen, Denmark

Abstract

Lhx9 is a member of the LIM homeobox gene family. It is expressed during mammalian embryogenesis in the brain including the pineal gland. Deletion of *Lhx9* results in sterility due to failure of gonadal development. The current study was initiated to investigate *Lhx9* biology in the pineal gland. *Lhx9* is highly expressed in the developing pineal gland of the rat with transcript abundance peaking early in development; transcript levels decrease postnatally to nearly undetectable levels in the adult, a temporal pattern that is generally similar to that reported for *Lhx9* expression in other brain regions. Studies with C57BL/6J $Lhx9^{-/-}$ mutant mice revealed marked alterations in brain and pineal development. Specifically, the superficial pineal gland is hypoplastic, being reduced to a small cluster of pinealocytes surrounded by meningeal and vascular tissue. The deep pineal gland and the pineal stalk are also reduced in size. Although the brains of neonatal $Lhx9^{-/-}$ mutant mice appear normal, severe hydrocephalus develops in about 70 % of the $Lhx9^{-/-}$ mice at 5–8 weeks of age; these observations are the first to document that deletion of *Lhx9* results in hydrocephalus and as such indicate that *Lhx9* contributes to the maintenance of normal brain structure. Whereas hydrocephalus is absent in neonatal $Lhx9^{-/-}$mutant mice, the neonatal pineal gland in these animals is hypoplastic. Accordingly, it appears that *Lhx9* is essential for early development of the mammalian pineal gland and that this effect is not secondary to hydrocephalus.

Keywords

Lhx9; Homeobox gene; Brain development; Pineal gland; Hydrocephalus

Introduction

Homeobox genes encode a large family of conserved transcription factors, which are involved in regulation of developmental processes, cellular differentiation and morphogenesis in all metazoans (McGinnis et al. 1984; Pearson et al. 2005). The pineal gland, a neuroendocrine organ converting photoperiodic information into the nocturnal hormonal signal of melatonin (Moller and Baeres 2002; Klein 2007), has been shown to express a number of homeobox genes both during development and postnatally (Rath et al. 2013). Pineal homeobox genes include members of the orthodenticle (Otx) and paired box (Pax) families (Rath et al. 2006, 2009); among these, *Pax6* and *Otx2* are known to be essential for pineal gland development (Nishida et al. 2003; Estivill-Torrus et al. 2001b), whereas the Otx-related cone–rod homeobox gene (*Crx*) exerts its function later in life by governing pineal-specific melatonin synthesis (Furukawa et al. 1999; Rovsing et al. 2011).

A less well-studied group of homeobox genes in the context of the pineal gland is the LIM homeobox (Lhx) gene family. Lhx genes are generally involved in tissue differentiation, especially neural patterning, in a variety of animal species (Hobert and Westphal 2000; Dawid and Chitnis 2001). In *Xenopus*, pineal expression of *Lhx2* (Viczian et al. 2006; Bachy et al. 2001) and *Lhx3* (Taira et al. 1993) has been reported. In rodents, *Lhx3* and *Lhx9* are expressed in the prenatal mouse pineal gland (Seidah et al. 1994; Retaux et al. 1999), whereas *Lhx4* transcripts are detectable in the adult rat pineal gland (Bailey et al. 2009); thus, Lhx genes may play currently unrecognized roles in pineal biology.

The *Lhx9* gene is widely expressed in the developing mouse forebrain including the epithalamic area (Retaux et al. 1999). *Lhx9* knockout animals have been generated by two groups (Birk et al. 2000; Wilson et al. 2008), using different targeting strategies. Studies using these animals have shown that this gene is essential for gonadal development (Birk et al. 2000) and development of a limited number of cell types in the central nervous system including projection neurons of the spinal cord (Wilson et al. 2008) and hypocretin-containing neurons of the hypothalamus (Dalal et al. 2013); however, knowledge on the role of *Lhx9* in development of the pineal gland is absent from the literature. To fill this gap in our knowledge of the role of *Lhx9* in pineal gland development, we investigated the developmental expression pattern of *Lhx9* in the rodent pineal gland and the pineal phenotype of the *Lhx9* knockout. In addition to discovering a role for this homeobox gene in pineal gland development, we also found that deletion of *Lhx9* causes severe hydrocephalus.

Materials and methods

Animals

Rat developmental series—For in situ hybridization experiments, Sprague–Dawley rats were obtained from timed pregnant mothers (Charles River, Sulzfeld, Germany). Animals were housed under a 12-h light, 12-h dark schedule (LD 12:12) at the Faculty of Health and Medical Sciences, University of Copenhagen, and decapitated at Zeitgeber time (ZT) 6 at the following developmental ages: embryonic day (E) 17, E18, E19, E20, E21, postnatal day (P) 2, P6, P12, P18 and P30. Heads or brains were fixed by immersion in 4 % paraformaldehyde, cryoprotected in 25 % sucrose and frozen on crushed solid CO_2. For the quantitative real-time reverse transcription PCR (qRT-PCR) and RNA-sequencing studies, Sprague–Dawley rats were obtained from timed pregnant mothers (Taconic Farms, Germantown, NY). Animals were housed for at least 2 weeks under a 14-h light, 10-h dark schedule (LD 14:10) at the Bethesda Campus, National Institutes of Health, before being killed by CO_2 asphyxiation and decapitated. Night procedures were done under dim red light. Pools of pineal glands (3–10 animals) were collected at ZT7 (E17, E19, E21, P2, P5, P10, P15, P20 and P40 for qRT-PCR; E21, P5, P20 and P40 for RNA sequencing) and at ZT19 (P2, P5, P10, P15, P20 and P40 for qRT-PCR; E21, P5, P20 and P40 for RNA sequencing), respectively. The pineal glands were frozen on solid CO_2.

Lhx9 knockout animals—*Lhx9*$^{+/-}$ heterozygous mice (Birk et al. 2000) that had been kept in a C57BL/6J background were provided by Dr. Heiner Westphal (NICHD, NIH). These animals were backcrossed to C57BL/6J wild-type mice to obtain heterozygous

animals, which were then backcrossed a second time with C57BL/6J wild-type mice. The resulting offspring were subsequently used for $(^{+/-}) \times (^{+/-})$ breeding to obtain *Lhx9*$^{-/-}$ animals.

Adult (6–8 weeks of age) and young (3 weeks of age, P21) animals were perfusion fixed with 4 % paraformaldehyde, and the heads were post-fixed by immersion in 4 % paraformaldehyde for 24 h. Fixed brains were removed from the skull, cryoprotected in 25 % sucrose and frozen on crushed solid CO_2.

Animal experiments were performed in accordance with the guidelines of EU Directive 86/609/EEC (approved by the Danish Council for Animal Experiments) and the National Institutes of Health Guide for Care and Use of Laboratory Animals (approved by the Governing Board of the National Research Council).

Genotyping

For DNA extraction, mouse tails were lysed in 180 μL of 50 mM NaOH by incubating at 95 °C for 2 h, followed by the addition of 20 μL of 1 M Tris–HCl (pH 8.0) and vortexing. 1 μL of lysate was used for a PCR reaction with KOD Xtreme Hot Start DNA Polymerase (Novagen, Madison, WI) according to the manufacturer's instructions. PCR across the *Lhx9* exon 2 and 3 splice junction was done with the following primers: 5′-ACG CCC CGA ACC CAC CCT CA-3′ and 5′-CAC CTG GCT GCT GCT TTC TGG G-3′. Primers used for PCR of the inserted PGK-NEO cassette and the *Lhx9* gene were 5′-GGG GTT GCC GTT CTG CCA GG-3′and 5′-ATC AGG ACA TAG CGT TGG CTA CC-3′.

RNA extraction

Total RNA was extracted with TRIzol reagent (Invitrogen, Carlsbad, CA), followed by cleanup using an RNeasy Micro Kit with on-column DNase treatment as per the manufacture's protocol (Qiagen, Valencia, CA). The amount and quality of RNA (RIN > 9) were determined using a NanoDrop spectrophotometer (NanoDrop, Wilmington, DE) and an Agilent 2100 Bioanalyzer (Agilent Technologies, Santa Clara, CA).

Quantitative real-time reverse transcription PCR

cDNA was synthesized from 500-ng DNase-treated total RNA by SuperScript III reverse transcriptase (Life Technologies, Grand Island, NY) using random hexamers. qRT-PCR was done using SYBR Green qPCR Mastermix (Qiagen, Valencia, CA) in a LightCycler 480 and the crossing points were calculated using the LightCycler™ software (Roche, Indianapolis, IN).

Primer sequences are given in Table 1. The PCR temperature profile was as follows: 95 °C for 10 min and then 45 cycles of 95 °C for 30 s, 60 °C for 30 s and 72 °C for 30 s. Product specificity was initially confirmed by agarose gel electrophoresis and direct sequencing, and melting curve analysis during every qRT-PCR thereafter. For each molecule, tenfold serial dilutions of each internal standard (10 fM to 1 nM) were used to generate a standard curve. Copy number values were normalized using a normalization factor calculated from the geometric mean of three reference gene transcripts, e.g., 28S ribosomal RNA (Rn28s1),

glyceraldehyde-3-phosphate dehydrogenase (Gapdh), and beta-actin (Actb), using geNorm (Vandesompele et al. 2002). The presented results are based on three independent experiments.

RNA sequencing

Total RNA (10 ug) was polyA-selected, fragmented, barcoded and four samples were run per sequencing lane on an Illumina HiSeq2000 machine, yielding an average of 39 million uniquely aligned paired-end 101-mer reads per sample (National Institutes of Health Intramural Sequencing Center). Reads were aligned to the reference rat genome (version rn4) using TopHat software, and expression levels were calculated as Fragments per Kilobase of transcript per Million reads (FPKM) using Cufflinks software (Trapnell et al. 2009, 2012; Roberts et al. 2011). Data are available from the National Center for Biotechnology Information Gene Expression Ominbus (http://www.ncbi.nlm.nih.gov/geo/) under accession number GSE46127.

Preparation of tissue for histology

Coronal cryostat sections of fixed and cryoprotected brains (20 μm) were mounted on Superfrost Plus glass slides (Menzel, Braunshweig, Germany), Nissl-stained in cresyl violet and cover-slipped in Pertex (Histolab, Gothenburg, Sweden). For each histological analysis, sections from at least three (3–5) animals of the same phenotype were examined.

Radiochemical in situ hybridization

Cryostat sections (14 μm) of fixed and cryoprotected brains were mounted on Superfrost Plus glass slides and hybridized with a ^{35}S-labeled DNA probe as previously described (Klitten et al. 2008; Rohde et al. 2011). For hybridization, the following probe, designed by use of Primer3 software (Untergasser et al. 2012) and manufactured commercially (DNA Technology, Århus, Denmark), was used: 5′-GAG AAC CTT CTG TAG TAA TCC TCC TTG CAG TAA ATG-3′ corresponding to position 485-450 on rat *Lhx9* mRNA (NM_181367.2). After hybridization and washing, the sections were exposed to an X-ray film for 2 weeks. Images on the X-ray film were transferred to a computer and quantified by the use of Scion Image Beta 4.0.2 (Scion Corporation, Frederick, MD). Optical densities from at least three parallel pineal sections from each animal were converted to dpm/mg tissue using simultaneously exposed ^{14}C-standards.

Immunohistochemistry

Coronal cryostat sections of fixed and cryoprotected brains (20 μm) were mounted on Superfrost Plus glass slides (Menzel, Braunshweig, Germany), and immunohistochemical reactions were performed as previously described (Rath et al. 2007). Sections were incubated with a rabbit anti-mouse S-antigen antiserum (Korf et al. 1985) diluted at 1:1000. Primary antisera were detected with a biotinylated secondary antiserum; chromogenic reactions were performed with ABC-Vectastain (Vector Laboratories, Burlingame, CA) and diaminobenzidine.

Statistical analyses

Quantitative data obtained by qRT-PCR or in situ hybridization were analyzed by use of GraphPad Prism 5.0 (GraphPad Software, La Jolla, CA). Data are presented as the mean ± standard error of mean (SEM). Data were analyzed by one-way analysis of variance (ANOVA) or two-way ANOVA followed by Bonferroni's multiple comparison post-test. A two-tailed p value of 0.05 was considered to represent statistical significance.

Results

Lhx9 is highly expressed in the prenatal pineal gland of the rat

The ontogenetic expression pattern of *Lhx9* in the developing pineal gland was examined by use of in situ hybridization in a developmental series of rats ranging from embryonic day (E) 17 to postnatal day (P) 30. At E17, the pineal gland is a small evagination from the caudal part of the diencephalic roof; however, the pineal recess was clearly identified with a high expression of *Lhx9* at this early stage (Fig. 1a). *Lhx9* transcripts were highly expressed in the prenatal pineal gland, but were undetectable in the postnatal gland. Hybridization signals were also detected in the mesencephalic tectum and in the thalamus at the early developmental stages (Fig. 1a), whereas *Lhx9* expression was not detected in the neopallium at any time examined. *Lhx9* expression was not detected in the brain of the adult rat. Densitometric analysis of pineal *Lhx9* expression confirmed that transcript abundance changed significantly during development (one-way ANOVA, $p < 0.0001$) with prenatal levels (E17–E19) being significantly higher than all expression levels detected at postnatal stages (Bonferroni's multiple comparison test, p values <0.001). The highest levels of pineal *Lhx9* expression were detected at E19.

qRT-PCR analysis of day and night samples of the developing rat pineal gland were in agreement with the in situ hybridization data and confirmed significant changes in pineal *Lhx9* expression during development (one-way ANOVA, $p < 0.0001$) with prenatal expression levels (E17–E21) exceeding all postnatal levels (Bonferroni's multiple comparison test, p values <0.01) (Fig. 2a), but failed to detect day/night differences in *Lhx9* transcript abundance at any of the examined postnatal stages (two-way ANOVA, $p = 0.70$) (Fig. 2a).

It was of interest to determine whether the marked developmental changes in *Lhx9* were seen also with other members of the LIM homeobox family. Previous studies have established that *Lhx4* is present in the adult rat pineal gland (Bailey et al. 2009). The current analysis revealed that *Lhx4* has a developmental expression pattern that is opposite to that of *Lhx9*; *Lhx4* increases around birth and remains highly expressed postnatally in the pineal gland with transcript abundance exceeding all prenatal levels (one-way ANOVA, $p < 0.0001$; Bonferroni's multiple comparison test, p values <0.0001); from P20, *Lhx4* exhibited a two-fold daily rhythm with high levels during night time (two-way ANOVA, $p < 0.0001$; Bonferroni's multiple comparison test, p values <0.0001) (Fig. 2a). The developmental pattern of other members of the LIM homeobox family in the pineal gland was analyzed by RNA sequencing (Fig. 2b); this revealed that *Isl2* was detectable at expression levels comparable to those of *Lhx4* and *Lhx9*, whereas other members were nearly undetectable.

Previous reports have determined that multiple *Lhx9* transcripts occur in vertebrates (Oshima et al. 2007; Failli et al. 2000; Smagulova et al. 2008). Here, we found that RNA-sequencing coverage plots (Coon et al. 2012) provide evidence that four *Lhx9* transcripts, corresponding to those previously reported in mammals, exist in the embryonic rat pineal gland; in addition, a novel 3′-terminal exon was discovered (Fig. 3).

Studies with *Lhx9*$^{-/-}$ mice

The transient pineal expression of *Lhx9* in the perinatal period led to the hypothesis that *Lhx9* was required for normal development of the pineal gland. Accordingly, we sought to determine whether elimination of *Lhx9* would alter development of the pineal gland. To accomplish this, we obtained *Lhx9* mutant C57BL/6J mice, which lack exon 2 and 3 of the gene (Birk et al. 2000). To generate homozygotes, heterozygote males and females were bred because homozygotes are sterile due to the absence of gonads. Litter size ranged from 4 to 8; the *Lhx9*$^{+/+}$:*Lhx9*$^{+/-}$:*Lhx9*$^{-/-}$ ratio was approximately 1:2:1. Pups appeared normal at birth.

Appearance of gross brain abnormalities with a severe hydrocephalic phenotype—By 8 weeks of age, a majority (approximately 70 %) of the *Lhx9*$^{-/-}$ mice exhibited severe hydrocephalus (Fig. 4). The age at which severe hydrocephalus first appeared was unpredictable, and in some cases there was no indication at 8 weeks of age. Twenty-five adult *Lhx9*$^{-/-}$ mice were examined, among these 17 were hydrocephalic and eight appeared normal. In contrast, hydrocephalus was not observed in the *Lhx9*$^{-/+}$ or wild-type C57BL/6J used in this study at any age, including 8 weeks and older.

In the hydrocephalic animals, the skull was malformed with a superior bulging of the calvarium, an incomplete broad sagittal suture and thin parietal and occipital bones. After removing the parietal and occipital bones, strongly dilated superior sagittal and transverse sinuses were observed. The confluence of sinuses was replaced by several abnormally dilated sinuses, and a proper superficial pineal gland was not macroscopically detectable. The brains were hydrocephalic with huge, enlarged lateral ventricles and a third ventricle, which was visible from the base of the brain (Fig. 4).

Coronal sections of the *Lhx9*$^{-/-}$ brains confirmed that the lateral and third ventricles were abnormally dilated (Fig. 5). The hypothalamus, thalamus and striatum were reduced in size, and the classical neuroanatomical nuclei were difficult to identify. Further, the neocortex was very thin and the normal six layers could not be identified (Figs. 5a, 6c). The brain stem and cerebellum appeared normal. The eyes, including the retina, were also developed normally (supplementary material, Fig. S1). The brains of both non-hydrocephalic adult *Lhx9*$^{-/-}$ animals and young knockout animals (P21) examined prior to the expected onset of hydrocephalus appeared macroscopically normal, and the neocortex exhibited a classical laminated morphology (Fig. 6) suggesting that the loss of lamination and the reduced thickness of the neocortex is a consequence of hydrocephalus.

Severe hypoplastic pineal complex—The wild-type rodent pineal organ consists of a deep pineal gland located on the dorsal part the brain stem between the habenular and posterior commissures. From the deep pineal, a stalk extends in caudal-superior direction

terminating in a larger superficial pineal gland located above the superior and inferior colliculi (Moller and Baeres 2002). In the adult *Lhx9*$^{-/-}$ brain, a deep pineal gland was present between the habenular commissure and a small posterior commissure, as visualized in coronal and sagittal sections. However, the size of the deep pineal was reduced. A very thin stalk with pial tissue and a few dispersed pinealocytes terminated caudally in a markedly underdeveloped superficial pineal gland located on the dorsal part of the mesencephalon. The superficial pineal tissue was surrounded by several sinuses and large veins (Fig. 7).

To investigate if the observed pineal hypoplasia was related to the hydrocephalic phenotype of the *Lhx9*$^{-/-}$ mouse, the epithalamus of young (P21) and non-hydrocephalic adult animals was examined. The abundance of pineal cells varied between animals, but even in these non-hydrocephalic *Lhx9*$^{-/-}$ animals, the superficial pineal gland was reduced to a small cluster of pinealocyte-like cells frequently dispersed in the surrounding meninges, and a proper pineal tissue with lobules and perivascular spaces was never observed (Fig. 8a, b). Examination of the deep pineal gland also revealed the presence of a reduced amount of deep pineal tissue in *Lhx9*$^{-/-}$ animals as compared to wild-type littermates (Fig. 8c, d). The morphology of the pineal complex of the young (P21) *Lhx9*$^{-/-}$ animal was found to be similar to that of the non-hydrocephalic adult phenotype indicating that pineal hypoplasia is not restricted to animals exhibiting hydrocephalus.

In an effort to determine whether the pineal cells in the *Lhx9*$^{-/-}$ mouse expressed the pinealocyte marker S-antigen, immunohistochemical studies were done. This revealed the presence of a limited number of S-antigen positive cells dispersed in meningeal tissue of the superficial pineal area (Fig. 9).

Discussion

This study has revealed that *Lhx9* plays a role in the development of the pineal gland and in maintenance of the brain structure. These two observations will be discussed in sequence below:

Lhx9 and pineal development

Normal pineal development requires a network of regulatory transcription factors, including a number of homeobox gene-encoded modulators, that have to be expressed in the developing pinealocyte in a timely coordinated manner (Rath et al. 2013). In the current study, we examined the pineal biology of *Lhx9*, a homeobox gene that has not previously been associated with pineal gland development. We have found that *Lhx9* plays a profound role in development of the rodent pineal organ and that in the absence of this homeobox gene, the pineal gland is hypoplastic.

As noted in the “Introduction”, pineal homeobox genes display different temporal patterns of expression (Rath et al. 2013). *Pax6* expression is restricted to prenatal stages, followed by *Otx2, Crx* and *Rax* (retina and anterior neural fold homeobox), which are expressed throughout development into adulthood, whereas *Pax4* is restricted to postnatal stages (Fig. 2b) (Rath et al. 2006, 2009; Rohde et al. 2011). This diversity appears to reflect different

functions in pinealocyte developmental processes and mature phenotype maintenance, as evidenced by the pineal phenotypes of available knockout animals (Nishida et al.2003; Furukawa et al. 1999; Estivill-Torrus et al. 2001b). The ontogenetic expression pattern of *Lhx9* in the rat pineal gland, with high prenatal expression followed by undetectable levels in the mature gland, suggests that this gene is primarily if not entirely involved in developmental processes and is not likely to be a part of adult pineal physiology. This is also the case with *Pax6*. PAX6 has been shown to cooperate with LHX2 in transcriptional activation of other homeobox genes during development of the retina (Tetreault et al. 2009). *Lhx2* and *Lhx9* are highly related structurally, but their spatial expression differs markedly, with *Lhx2* expressed in the mammalian retina whereas *Lhx9* transcripts occur in the pineal gland (Retaux et al. 1999). The pinealocyte of the pineal gland and the retinal photoreceptor are two closely related cell types (Klein 2004) and their transcriptomes share many genes highly enriched only in these two tissues (Bailey et al. 2009). However, in this case *Lhx2* is restricted to the developing retina (Retaux et al. 1999; Porter et al. 1997), whereas *Lhx9* is the pineal ortholog; therefore, it is possible that LHX9 is the cooperating partner of PAX6 during pineal development. In contrast, pineal expression of *Lhx4*, like that of *Pax4* (Rath et al. 2009), increases postnatally and even exhibits a daily rhythm, which may suggest that *Lhx4* is involved in postnatal circadian biology of the pineal gland rather than developmental processes, thus adding to the complexity of the roles of LIM homeobox genes in the pineal gland.

Lhx9 transcripts were also detected prenatally in the thalamus and in the mesencephalic tectum. A previous study on *Lhx9* expression in the developing brain of the mouse has shown that the gene is more widely expressed at earlier stages with the early *Lhx9* expression domain covering large parts of the forebrain including the neopallium (Retaux et al. 1999). In the mouse, neocortical expression ceases around E15, whereas expression in more caudal parts of the brain, including the thalamus and mesencephalic tectum, persists until perinatal stages (Retaux et al. 1999). Thus, our in situ hybridization data on the rat starting at E17 are in full agreement with these previous findings.

The functional importance of *Lhx9* in development of the pineal gland is evident from the pineal phenotype of $Lhx9^{-/-}$ mice. In these animals, the pineal gland is reduced to a small cluster of superficial pineal cells surrounded by pial tissue above the inferior colliculi and a few deep pineal cells around the habenular commissure. However, the superficial part of the pineal complex of the $Lhx9^{-/-}$ brain is devoid of normal pineal glandular morphology characterized by lobules and perivascular spaces. Thus, our data establish that *Lhx9* is essential for development of the rodent pineal gland. This developmental role is in agreement with the early expression of *Lhx9* in the pineal recess.

Our immunohistochemical analyses have revealed that the few pineal cells present in the $Lhx9^{-/-}$ mice were S-antigen positive. S-antigen is a pinealocyte marker and is detectable only postnatally in the rodent pineal gland (Babila et al. 1992) indicating that the $Lhx9^{-/-}$ pineal cells, also from a molecular point of view, should be regarded as dispersed pinealocytes and not as remnants of early pinealocyte-progenitors. Our data suggest that *Lhx9* contributes to early proliferation, specification or survival of pinealocytes or a combination. On the other hand, our findings that the few pinealocytes present are found in

both the superficial and deep part of a severely reduced pineal organ indicates that the developmental migration and gross anatomical subdivision of pinealocytes are not compromised by the lack *Lhx9*, rather it would appear that *Lhx9* governs the development of the pineal cell per se.

As noted in the "Introduction", *Pax6* and *Otx2* have been previously shown to be essential for pineal gland development (Nishida et al. 2003; Estivill-Torrus et al. 2001b); however, the data presented in these previous reports do not exclude the possibility that *Pax6* and *Otx2* deletions may also allow development of a limited number of pinealocytes. Both *Pax6* and *Otx2* are also required for proper development of the neural retina (Grindley et al. 1995; Gehring 1996; Nishida et al. 2003); however, the $Lhx9^{-/-}$ mice do not display retinal abnormalities, showing that in this pineal–retinal context, the role of *Lhx9* is pineal-specific. Interestingly, a hypoplastic pineal gland was also reported in a brain-specific homeobox gene (*Bsx*) knockout mouse (McArthur and Ohtoshi 2007), suggesting that *Bsx* and *Lhx9* may control similar developmental processes in the early pinealocyte.

Lhx9 and hydrocephalus

This study has revealed that severe hydrocephalus occurs in the brain of the adult $Lhx9^{-/-}$ C57BL/6J mouse, adding to previous reports on the effects that *Lhx9* deletion has on gonadal development (Birk et al. 2000) and on specific neuronal cell subtypes of the central nervous system (Wilson et al. 2008; Dalal et al. 2013).

We observed that the majority *Lhx9* knockout mice displayed late-onset hydrocephalus, which we suspect is due to closure or occlusion of the cerebral aqueduct of Sylvius connecting the third ventricle with the fourth ventricle through the mesencephalon, thus increasing the pressure in the rostral ventricular system. The dilated lateral ventricles, the opening in the bottom of the third ventricle and the normal development of brain structures caudal to the mesencephalon support this interpretation. The relatively late development of hydrocephalus may be explained by a slowly progressing pathophysiology or a persistent role of *Lhx9* in the mesencephalon as evidenced by postnatal expression in this brain area (Retaux et al. 1999). *Pax6* mutant mice, which also fail to develop the pineal gland, exhibit congenital hydrocephalus (Estivill-Torrus et al. 2001a, b). However, an etiological connection between the hydrocephalic phenotypes of *Pax6* and *Lhx9* mutants seems unlikely, since hydrocephalus in the *Pax6* mutants has been attributed to lack of the subcommissural organ (Estivill-Torrus et al. 2001a), which is present in $Lhx9^{-/-}$ brain (Fig. 8d). It is possible that the mixed phenotype of the *Lhx9* knockout mouse is associated with different degrees of passage through the cerebral aqueduct resulting in different pressure gradients and accordingly a variable size of the ventricular system affecting the development of periventricular structures. In this regard, our data suggest that the lack of neocortical lamination is a consequence of the dilation of the underlying lateral ventricles and is not caused directly by the lack of *Lhx9* in the neopallium itself, although it is expressed in this part of the brain early in development (Retaux et al. 1999).

It is puzzling that hydrocephalus has not been previously observed in $Lhx9^{-/-}$ mice (Birk et al. 2000; Dalal et al. 2013; Wilson et al. 2008). This may reflect the fact that hydrocephalus develops postnatally and that prior studies focused on earlier developmental stages. Another

possibility is that genetic background plays a role in hydrocephalus. In support of this is the observation of a more frequent penetrance of hydrocephalus in *Lhx9*$^{-/-}$ mice (Wilson et al. 2008) after crossing into a C57BL/6J background (Dr. Joseph D. Dougherty, Washington University, personal communication). This evidence of a greater potential for C57BL/6J mice to develop hydrocephalus is in agreement with work on JAM-C mutants, in which hydrocephalus is seen against a C57BL/6J background but not against a mixed background (Wyss et al. 2012). Accordingly, it is possible that genetic elements present in the founding chimeric *Lhx9*$^{-/-}$ mice were not fully bred out after being backcrossed into the C57BL/6J line in previous studies (Birk et al. 2000) and that those animals retained a genetic profile which masked the effects of *Lhx9* deletion through functional redundancy. The tendency of C57BL/6J mice to develop hydrocephalus has been discussed previously (Wyss et al. 2012). In addition, our finding that hydrocephalus did not develop in all the *Lhx9*$^{-/-}$ mice may also be explained by the influence of remaining non-C57BL/6J gene elements.

A number of loci have been associated with the development of hydrocephalus in mammals (Zhang et al. 2006). The findings of the studies presented here add *Lhx9* to the list of genes that are involved in normal brain development. Our observations support the interpretation that hydrocephalus can result from a mutation in one of several genes acting via different neuropathologies. The growing indication that C57BL/6J mice are, especially prone to development of hydrocephalus, suggests that this line lacks genetic redundancy or “genetic insurance” that otherwise prevents this abnormality; identification of this deficiency would be of broad interest.

Supplementary Material

Refer to Web version on PubMed Central for supplementary material.

Acknowledgments

This study was supported by the Intramural Research Program of the *Eunice Kennedy Shriver* National Institute of Child Health and Human Development of the National Institutes of Health and the Lundbeck Foundation (grant number R108-A10301). We are grateful to Dr. Heiner Westphal’s (NICHD) gift of the *Lhx9*$^{-/-}$ mice and for the support provided by Dr. Yangu Zhao (NICHD) in establishing a colony of *Lhx9* mutant mice. We recognize the full value of the willingness of Dr. Joseph D. Dougherty, Washington University, to share unpublished observations. The expertise and dedication of Daniel Abebe as applied to the expansion and management of the mutant *Lhx9* colony in our facilities, which was essential to the success of this investigation, is greatly valued.

Abbreviations

Actb	Beta-actin
Bsx	Brain-specific homeobox
Crx	Cone–rod homeobox
E	Embryonic day
Gapdh	Glyceraldehyde-3-phosphate dehydrogenase
LD	Light–dark schedule
Lhx	LIM homeobox

Otx	Orthodenticle homeobox
P	Postnatal day
Pax	Paired box
qRT-PCR	Quantitative real-time reverse transcription PCR
Rax	Retina and anterior neural fold homeobox
Rn28s1	28S ribosomal RNA
ZT	Zeitgeber time

References

Babila T, Schaad NC, Simonds WF, Shinohara T, Klein DC. Development of MEKA (phosducin), G beta, G gamma and S-antigen in the rat pineal gland and retina. Brain Res. 1992; 585(1–2):141–148. [PubMed: 1511297]

Bachy I, Vernier P, Retaux S. The LIM-homeodomain gene family in the developing Xenopus brain: conservation and divergences with the mouse related to the evolution of the forebrain. J Neurosci. 2001; 21(19):7620–7629. [PubMed: 11567052]

Bailey MJ, Coon SL, Carter DA, Humphries A, Kim JS, Shi Q, Gaildrat P, Morin F, Ganguly S, Hogenesch JB, Weller JL, Rath MF, Moller M, Baler R, Sugden D, Rangel ZG, Munson PJ, Klein DC. Night/day changes in pineal expression of >600 genes: central role of adrenergic/cAMP signaling. J Biol Chem. 2009; 284(12):7606–7622. doi:10.1074/jbc.M808394200. [PubMed: 19103603]

Birk OS, Casiano DE, Wassif CA, Cogliati T, Zhao L, Zhao Y, Grinberg A, Huang S, Kreidberg JA, Parker KL, Porter FD, Westphal H. The LIM homeobox gene Lhx9 is essential for mouse gonad formation. Nature. 2000; 403(6772):909–913. doi:10.1038/35002622. [PubMed: 10706291]

Coon SL, Munson PJ, Cherukuri PF, Sugden D, Rath MF, Moller M, Clokie SJ, Fu C, Olanich ME, Rangel Z, Werner T, Mullikin JC, Klein DC. Circadian changes in long noncoding RNAs in the pineal gland. Proc Natl Acad Sci USA. 2012; 109(33):13319–13324. doi:10.1073/pnas.1207748109. [PubMed: 22864914]

Dalal J, Roh JH, Maloney SE, Akuffo A, Shah S, Yuan H, Wamsley B, Jones WB, Strong Cde G, Gray PA, Holtzman DM, Heintz N, Dougherty JD. Translational profiling of hypocretin neurons identifies candidate molecules for sleep regulation. Genes Dev. 2013; 27(5):565–578. doi:10.1101/gad.207654.112. [PubMed: 23431030]

Dawid IB, Chitnis AB. Lim homeobox genes and the CNS: a close relationship. Neuron. 2001; 30(2):301–303. [PubMed: 11394990]

Estivill-Torrus G, Lopez-Aranda MF, Grondona JM, Bach A, Robert B, Vitalis T, Price DJ, Ramos C, Soriano E, Fernandez-Llebrez P. Pax6 and Msx1, two homeobox genes involved in the development of the subcommissural organ. Int J Dev Biol. 2001a; 45(S1):S75–S76.

Estivill-Torrus G, Vitalis T, Fernandez-Llebrez P, Price DJ. The transcription factor Pax6 is required for development of the diencephalic dorsal midline secretory radial glia that form the subcommissural organ. Mech Dev. 2001b; 109(2):215–224. [PubMed: 11731235]

Failli V, Rogard M, Mattei MG, Vernier P, Retaux S. Lhx9 and Lhx9alpha LIM-homeodomain factors: genomic structure, expression patterns, chromosomal localization, and phylogenetic analysis. Genomics. 2000; 64(3):307–317. doi:10.1006/geno.2000.6123. [PubMed: 10756098]

Furukawa T, Morrow EM, Li T, Davis FC, Cepko CL. Retinopathy and attenuated circadian entrainment in Crxdeficient mice. Nat Genet. 1999; 23(4):466–470. doi:10.1038/70591. [PubMed: 10581037]

Gehring WJ. The master control gene for morphogenesis and evolution of the eye. Genes Cells. 1996; 1(1):11–15. [PubMed: 9078363]

Grindley JC, Davidson DR, Hill RE. The role of Pax-6 in eye and nasal development. Development. 1995; 121(5):1433–1442. [PubMed: 7789273]

Hobert O, Westphal H. Functions of LIM-homeobox genes. Trends Genet. 2000; 16(2):75–83. [PubMed: 10652534]

Klein DC. The 2004 Aschoff/Pittendrigh lecture: theory of the origin of the pineal gland—a tale of conflict and resolution. J Biol Rhythms. 2004; 19(4):264–279. doi:10.1177/0748730404267340. [PubMed: 15245646]

Klein DC. Arylalkylamine *N*-acetyltransferase: "the Time-zyme". J Biol Chem. 2007; 282(7):4233–4237. doi:10.1074/jbc.R600036200. [PubMed: 17164235]

Klitten LL, Rath MF, Coon SL, Kim JS, Klein DC, Moller M. Localization and regulation of dopamine receptor D4 expression in the adult and developing rat retina. Exp Eye Res. 2008; 87(5): 471–477. doi:10.1016/j.exer.2008.08.004. [PubMed: 18778704]

Korf HW, Moller M, Gery I, Zigler JS, Klein DC. Immunocytochemical demonstration of retinal S-antigen in the pineal organ of four mammalian species. Cell Tissue Res. 1985; 239(1):81–85. [PubMed: 3967288]

McArthur T, Ohtoshi A. A brain-specific homeobox gene, Bsx, is essential for proper postnatal growth and nursing. Mol Cell Biol. 2007; 27(14):5120–5127. doi:10.1128/MCB.00215-07. [PubMed: 17485440]

McGinnis W, Garber RL, Wirz J, Kuroiwa A, Gehring WJ. A homologous protein-coding sequence in *Drosophila* homeotic genes and its conservation in other metazoans. Cell. 1984; 37(2):403–408. [PubMed: 6327065]

Moller M, Baeres FM. The anatomy and innervation of the mammalian pineal gland. Cell Tissue Res. 2002; 309(1):139–150. doi:10.1007/s00441-002-0580-5. [PubMed: 12111544]

Nishida A, Furukawa A, Koike C, Tano Y, Aizawa S, Matsuo I, Furukawa T. Otx2 homeobox gene controls retinal photoreceptor cell fate and pineal gland development. Nat Neurosci. 2003; 6(12): 1255–1263. doi:10.1038/nn1155. [PubMed: 14625556]

Oshima Y, Noguchi K, Nakamura M. Expression of Lhx9 isoforms in the developing gonads of Rana rugosa. Zoolog Sci. 2007; 24(8):798–802. [PubMed: 18217486]

Pearson JC, Lemons D, McGinnis W. Modulating Hox gene functions during animal body patterning. Nat Rev Genet. 2005; 6(12):893–904. doi:10.1038/nrg1726. [PubMed: 16341070]

Porter FD, Drago J, Xu Y, Cheema SS, Wassif C, Huang SP, Lee E, Grinberg A, Massalas JS, Bodine D, Alt F, Westphal H. Lhx2, a LIM homeobox gene, is required for eye, forebrain, and definitive erythrocyte development. Development. 1997; 124(15):2935–2944. [PubMed: 9247336]

Rath MF, Munoz E, Ganguly S, Morin F, Shi Q, Klein DC, Moller M. Expression of the Otx2 homeobox gene in the developing mammalian brain: embryonic and adult expression in the pineal gland. J Neurochem. 2006; 97(2):556–566. doi:10.1111/j.1471-4159.2006.03773.x. [PubMed: 16539656]

Rath MF, Morin F, Shi Q, Klein DC, Moller M. Ontogenetic expression of the *Otx2* and *Crx* homeobox genes in the retina of the rat. Exp Eye Res. 2007; 85(1):65–73. doi:10.1016/j.exer.2007.02.016. [PubMed: 17467693]

Rath MF, Bailey MJ, Kim JS, Ho AK, Gaildrat P, Coon SL, Moller M, Klein DC. Developmental and diurnal dynamics of Pax4 expression in the mammalian pineal gland: nocturnal down-regulation is mediated by adrenergic-cyclic adenosine 3′,5′-monophosphate signaling. Endocrinology. 2009; 150(2):803–811. doi:10.1210/en.2008-0882. [PubMed: 18818287]

Rath MF, Rohde K, Klein DC, Moller M. Homeobox genes in the rodent pineal gland: roles in development and phenotype maintenance. Neurochem Res. 2013; 38(6):1100–1112. doi:10.1007/s11064-012-0906-y. [PubMed: 23076630]

Retaux S, Rogard M, Bach I, Failli V, Besson MJ. Lhx9: a novel LIM-homeodomain gene expressed in the developing forebrain. J Neurosci. 1999; 19(2):783–793. [PubMed: 9880598]

Roberts A, Pimentel H, Trapnell C, Pachter L. Identification of novel transcripts in annotated genomes using RNA-Seq. Bioinformatics. 2011; 27(17):2325–2329. doi:10.1093/bioinformatics/btr355. [PubMed: 21697122]

Rohde K, Klein DC, Moller M, Rath MF. Rax: developmental and daily expression patterns in the rat pineal gland and retina. J Neurochem. 2011; 118(6):999–1007. doi:10.1111/j.1471-4159.2011.07385.x. [PubMed: 21749377]

Rovsing L, Clokie S, Bustos DM, Rohde K, Coon SL, Litman T, Rath MF, Moller M, Klein DC. Crx broadly modulates the pineal transcriptome. J Neurochem. 2011; 119(2):262–274. doi:10.1111/j.1471-4159.2011.07405.x. [PubMed: 21797868]

Seidah NG, Barale JC, Marcinkiewicz M, Mattei MG, Day R, Chretien M. The mouse homeoprotein mLIM-3 is expressed early in cells derived from the neuroepithelium and persists in adult pituitary. DNA Cell Biol. 1994; 13(12):1163–1180. [PubMed: 7811383]

Smagulova FO, Manuylov NL, Leach LL, Tevosian SG. GATA4/FOG2 transcriptional complex regulates Lhx9 gene expression in murine heart development. BMC Dev Biol. 2008; 8:67. doi:10.1186/1471-213X-8-67. [PubMed: 18577233]

Taira M, Hayes WP, Otani H, Dawid IB. Expression of LIM class homeobox gene *Xlim-3* in Xenopus development is limited to neural and neuroendocrine tissues. Dev Biol. 1993; 159(1):245–256. doi:10.1006/dbio.1993.1237. [PubMed: 8103491]

Tetreault N, Champagne MP, Bernier G. The LIM homeobox transcription factor Lhx2 is required to specify the retina field and synergistically cooperates with Pax6 for Six6 trans-activation. Dev Biol. 2009; 327(2):541–550. doi:10.1016/j.ydbio.2008.12.022. [PubMed: 19146846]

Trapnell C, Pachter L, Salzberg SL. TopHat: discovering splice junctions with RNA-Seq. Bioinformatics. 2009; 25(9):1105–1111. doi:10.1093/bioinformatics/btp120. [PubMed: 19289445]

Trapnell C, Roberts A, Goff L, Pertea G, Kim D, Kelley DR, Pimentel H, Salzberg SL, Rinn JL, Pachter L. Differential gene and transcript expression analysis of RNA-seq experiments with TopHat and Cufflinks. Nat Protoc. 2012; 7(3):562–578. doi:10.1038/nprot.2012.016. [PubMed: 22383036]

Untergasser A, Cutcutache I, Koressaar T, Ye J, Faircloth BC, Remm M, Rozen SG. Primer3—new capabilities and interfaces. Nucleic Acids Res. 2012; 40(15):e115. doi:10.1093/nar/gks596. [PubMed: 22730293]

Vandesompele J, De Preter K, Pattyn F, Poppe B, Van Roy N, De Paepe A, Speleman F. Accurate normalization of real-time quantitative RT-PCR data by geometric averaging of multiple internal control genes. Genome Biol. 2002; 3(7) RESEARCH0034.

Viczian AS, Bang AG, Harris WA, Zuber ME. Expression of *Xenopus laevis* Lhx2 during eye development and evidence for divergent expression among vertebrates. Dev Dyn. 2006; 235(4):1133–1141. doi:10.1002/dvdy.20708. [PubMed: 16470628]

Wilson SI, Shafer B, Lee KJ, Dodd J. A molecular program for contralateral trajectory: rig-1 control by LIM homeodomain transcription factors. Neuron. 2008; 59(3):413–424. doi:10.1016/j.neuron.2008.07.020. [PubMed: 18701067]

Wyss L, Schafer J, Liebner S, Mittelbronn M, Deutsch U, Enzmann G, Adams RH, Aurrand-Lions M, Plate KH, Imhof BA, Engelhardt B. Junctional adhesion molecule (JAM)-C deficient C57BL/6 mice develop a severe hydrocephalus. PLoS One. 2012; 7(9):e45619. doi:10.1371/journal.pone.0045619. [PubMed: 23029139]

Zhang J, Williams MA, Rigamonti D. Genetics of human hydrocephalus. J Neurol. 2006; 253(10):1255–1266. doi:10.1007/s00415-006-0245-5b. [PubMed: 16773266]

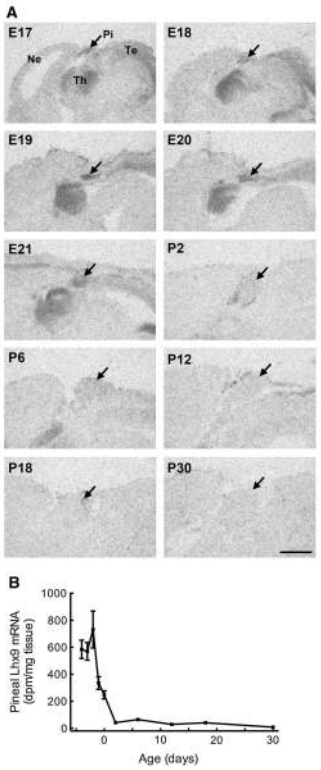

Fig. 1.

Radiochemical in situ hybridization for detection of *Lhx9* in the developing rat brain. **a** Autoradiographs of hybridized sagittal sections of the developing brain. The pineal (Pi) is indicated by the *arrow*. There is also a signal in the mesencephalic tectum (Te) and the thalamus (Th) at the early developmental stages. The neopallium (Ne) is negative, but labeled for orientation purposes. *Scale bar* 1 mm. **b** Densitometric quantification of *Lhx9* mRNA in the developing rat pineal gland. Each value on *graph* represents the mean ± SEM of three different animals

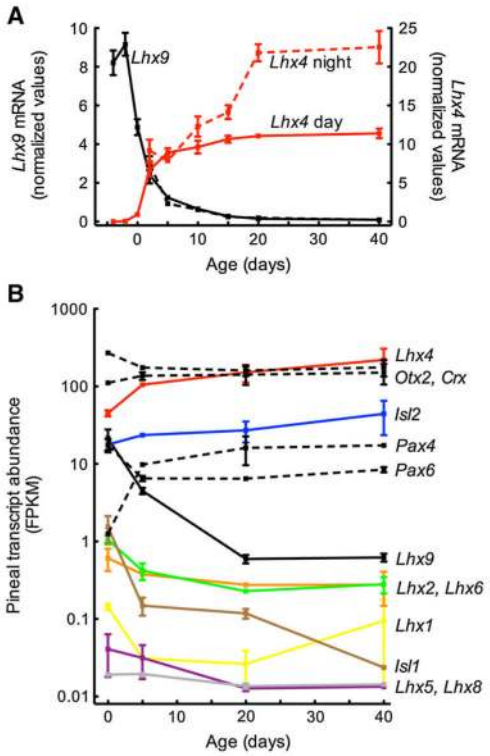

Fig. 2.

Developmental and daily expression of *Lhx9* and *Lhx4* in the rat pineal gland. **a** qRT-PCR analysis of *Lhx4* and *Lhx9* expression in the rat pineal gland. Both prenatal and postnatal pineal glands were removed during daytime (ZT7, *solid line*) and nighttime (ZT19, *dashed line*). Each value on graph represents the mean ± SEM of three different pools of glands. **b** RNA-seq analysis of LIM homeobox gene expression in the developing rat pineal gland. Values on *graph* represent the mean with range of two FPMK values from different pools of glands obtained during daytime (ZT7) and nighttime (ZT19); therefore, note that daytime and nighttime samples are not represented by *separate lines* in (**b**). For comparison, the ontogenetic expression profiles of homeobox genes of the paired box (*Pax4* and *Pax6*) and orthodenticle (*Otx2* and *Crx*) families are displayed (*dashed lines*). *Crx* cone–rod homeobox, *Lhx* LIM homeobox, *Isl* islet, *Otx* orthodenticle homeobox, *Pax* paired box

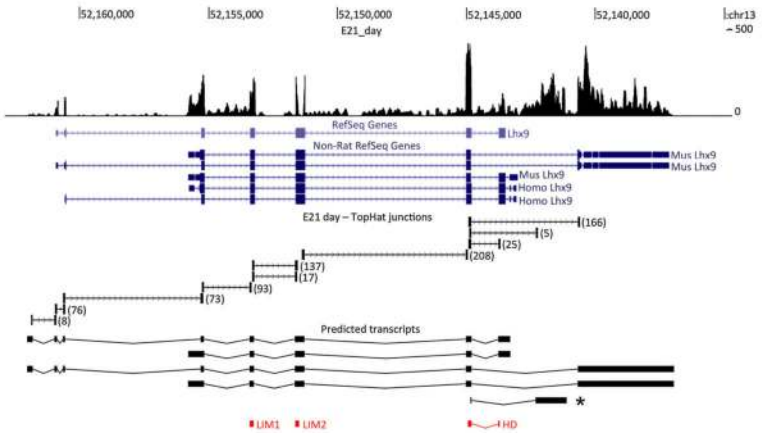

Fig. 3.

The genomic structure of *Lhx9* transcripts in the rat pineal gland. The histogram shows the RNA-seq coverage plot for a pineal E21 day sample viewed in the UCSC Browser. The numbers across the top indicate the location on chromosome 13. The tracks for rat, mouse and human RefSeq entries are shown in *blue*. Below them are indicated the splice junctions found in the RNA-seq data by Tophat; the *numbers* indicate the number of times the junction was found in the E21 day sample. Next are shown the four predicted splice variants. Analogs of these have been previously cloned and annotated from rat, mouse or human. In addition, a novel annotated terminal exon (*asterisk*) is displayed. At the bottom are shown the locations of the conserved domains

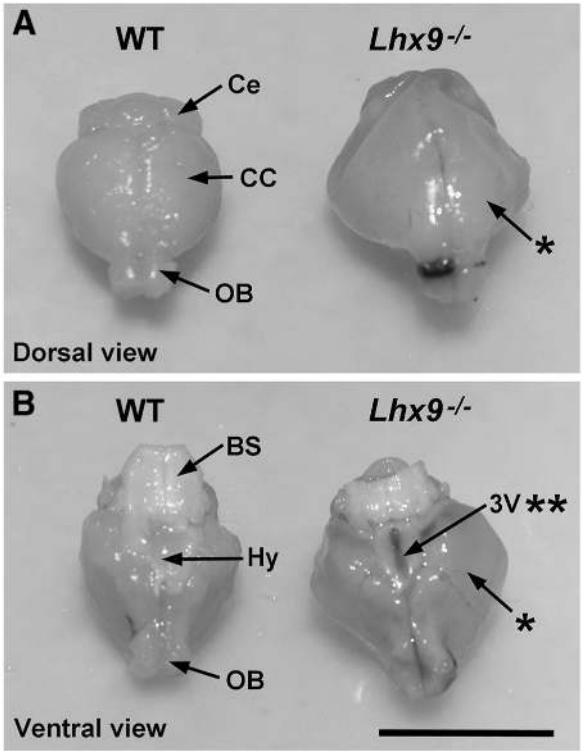

Fig. 4.

Gross anatomy of the brain of the *Lhx9* knockout mouse. Photographs of a brain from an adult *Lhx9* knockout mouse (*Lhx9*$^{-/-}$) compared to a wild-type littermate (WT) viewed from the ventral (**a**) and dorsal (**b**) side, respectively. *BS* brain stem, *CC* cerebral cortex, *Ce*, cerebellum, *Hy* hypothalamus, *OB* olfactory bulb, *, note the hydrocephalic forebrain; **, note the abnormal ventral opening of the hypothalamus. *Scale bar* 1 cm

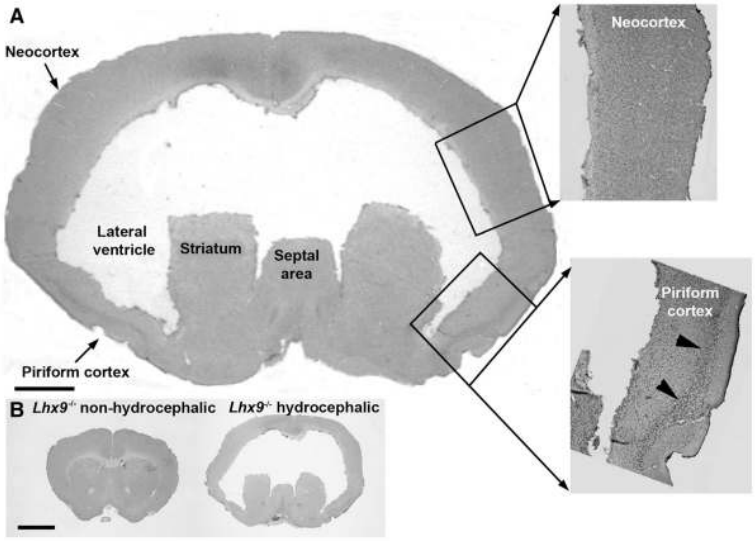

Fig. 5.

Histology of the brain of the hydrocephalic *Lhx9*$^{-/-}$ mouse. **a** Coronal Nissl-stained section through the septal area of the brain of a hydrocephalic 6-week-old *Lhx9*$^{-/-}$ mouse. Huge dilatations of the lateral and third ventricles and thinning of the cerebral hemispheres are seen. There is no cortical lamination of the neocortex (insert: neocortex), but in the piriform cortex, the granular layer is clearly detectable (*arrow head* in the insert: piriform cortex). *Scale bar* 1 mm. **b** Coronal Nissl-stained section through the septal area of a morphologically normal non-hydrocephalic *Lhx9*$^{-/-}$ mouse brain (*left*) and a hydrocephalic *Lhx9*$^{-/-}$ mouse brain (*right*). *Scale bar* 2 mm

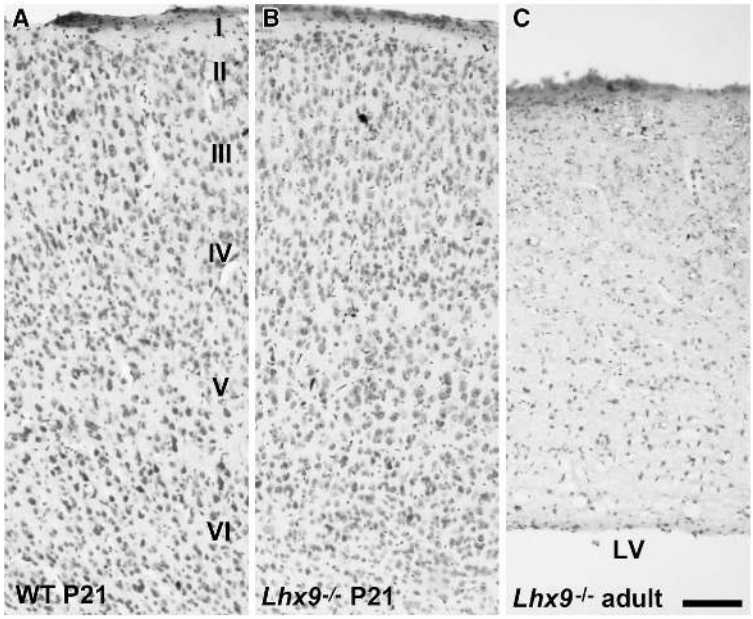

Fig. 6.

Histology of the neocortex of the young non-hydrocephalic *Lhx9*$^{-/-}$ mouse. Coronal Nissl-stained sections through the neocortex of a P21 *Lhx9*$^{-/-}$ mouse (**b**) and a wild-type littermate (**a**). In both genotypes, the neocortex appears normal exhibiting the characteristic six-layered pattern. *Roman numerals* indicate neocortical layers. For comparison, a section of the neocortex of a hydrocephalic adult *Lhx9*$^{-/-}$ mouse is displayed (c). *LV* lateral ventricle. *Scale bar* 100 μm

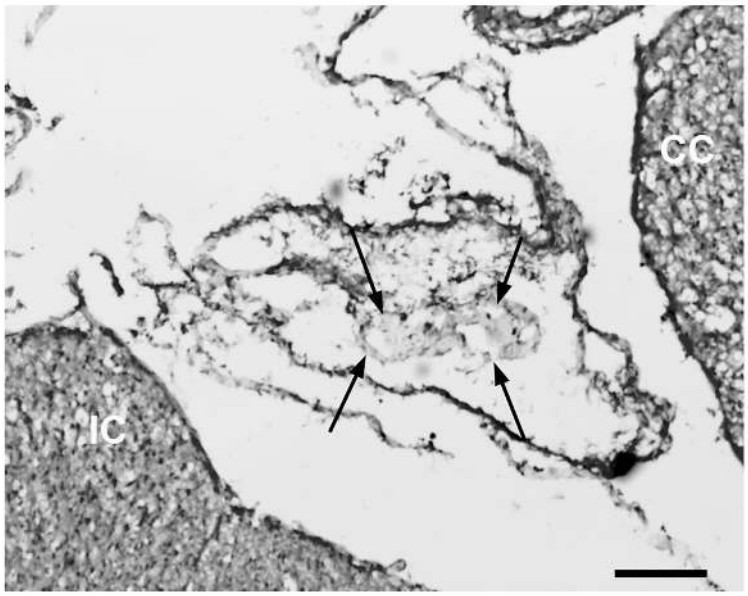

Fig. 7.

Histology of the superficial pineal gland of the hydrocephalic *Lhx9*$^{-/-}$ mouse. Coronal Nissl-stained section through the superficial pineal tissue of a hydrocephalic *Lhx9* knockout mouse (8 weeks of age). The margins of a cluster of pineal cells surrounded by meningeal and venous tissues are delineated by *arrows*. Notably, the pineal gland is devoid of the lobules and perivascular spaces that typify the tissue. *CC* cerebral cortex, *IC* inferior colliculus. *Scale bar* 500 μm

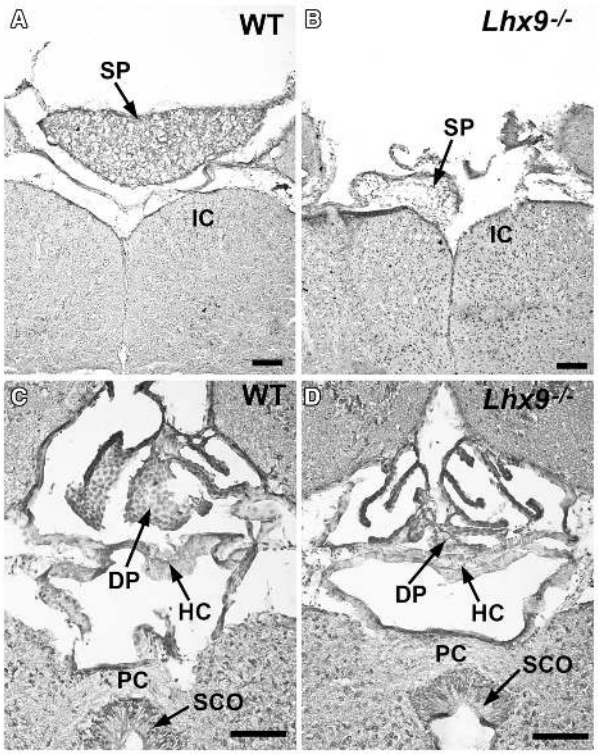

Fig. 8.

Histology of the hypoplastic pineal complex of the young non-hydrocephalic *Lhx9*$^{-/-}$ mouse. Nissl-stained coronal sections of the superficial pineal gland of a wild-type (**a**), the area of the superficial pineal gland of an *Lhx9*$^{-/-}$ mouse (**b**), the deep pineal gland of a wild-type (**c**) and the same area of an *Lhx9*$^{-/-}$ mouse (**d**). Displayed images were all obtained from non-hydrocephalic littermates killed at P21. Note the lack of a proper superficial (**b**) and deep (**d**) pineal gland in the *Lhx9* knockout. *DP* deep pineal gland, *HC* habenular commissure, *IC* inferior colliculus, *PC* posterior commissure, *SCO* subcommissural organ, *SP* superficial pineal gland. *Scale bars* 100 μm

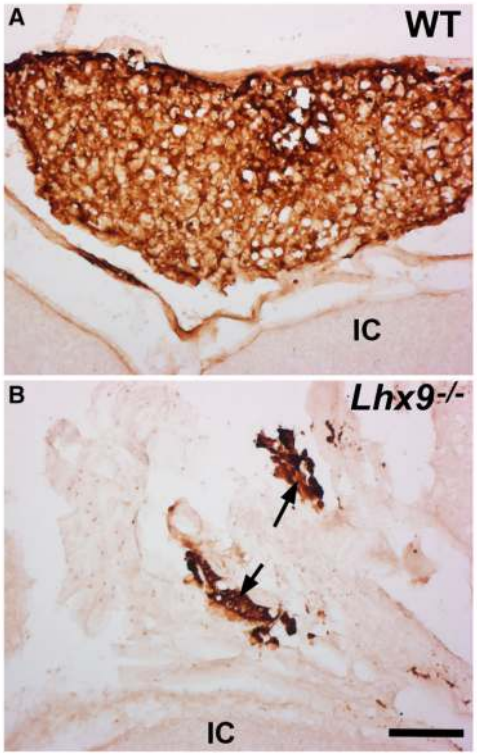

Fig. 9.

Immunohistochemical staining for detection of S-antigen in the superficial pineal gland of the *Lhx9*$^{-/-}$ mouse. Immunoreacted coronal sections of the superficial pineal gland of a wild-type mouse (**a**) and the corresponding area of an *Lhx9*$^{-/-}$ mouse (**b**). Animals were killed at P21. *Arrows* indicate dispersed immunoreactive pinealocytes surrounded by meningeal tissue in the *Lhx9*$^{-/-}$ mouse. *IC* inferior colliculus. *Scale bar* 100 μm

Table 1

Sequences of primers used for qRT-PCR analyses

Transcript	Forward primer (5′–3′)	Reverse primer (5′–3′)
Lhx4	CAGATCCTTCCCCTGACCT	AGACTTGAGGCAGGAGCTGT
Lhx9	GCGCGGTCCGCTACTCTTGC	CGGGGGCATACCCGCGTCG
Actb	ACGGTCAGGTCATCACTATCG	AGCCACCAATCCACACAGA
Gapdh	TGGTGAAGGTCGGTGTGAACGGAT	TCCATGGTGGTGAAGACGCCAGTA
Rn28s1	TTGAAAATCCGGGGGAGAG	ACATTGTTCCAACATGCCAG